

## Article

# Diverse CT Findings of Pulmonary Infection in Patients with Kidney Diseases under Immunosuppressive Therapy or on Maintenance Hemodialysis

Shuai Zhou <sup>1,2†</sup>, XiaoMing Liu <sup>1†</sup>, PeiHua Hu <sup>3</sup>, HuiNing Liu <sup>4</sup>, Yong Wang <sup>5</sup>, LiHong Zhang <sup>1</sup> and Tao Wang <sup>1,\*</sup>

<sup>1</sup> Graduate School of HeBei Medical University, 050011 Shijiazhuang, P.R. China

<sup>2</sup> Department of Nephrology

<sup>4</sup> Department of Thoracic Surgery

<sup>5</sup> Department of Medical Imaging, the First Hospital of HeBei Medical University, 050030 Shijiazhuang, P.R. China

†These authors contributed equally to this work

\*Corresponding author: nephrology2009@hotmail.com; Tel.: +86-18632191726

**Abstract:** Patients under immunosuppressive therapy for kidney diseases or on maintenance hemodialysis are more susceptible to infection than the general population since loss of renal function *per se* was an immunocompromised condition. Of relevance, CT imaging plays a crucial role in the detection and management of pulmonary infectious diseases. We hence presented diverse CT findings of pulmonary infections in the above said patients collected during our arduous work against a wide range of pathogens including *klebsiella pneumoniae*, *staphylococcus aureus*, *candida parapsilosis*, *aspergillus*, *cryptococcus*, *mucor*, *pneumocystis carinii*, *cytomegalovirus*, *mycobacterium* and *nocardia*. Notably, the pulmonary pathological changes were either primary pneumonia or secondary to the catheter-associated bloodstream infection. For a descriptive purpose, pulmonary manifestations of Wegener's granuloma, lung cancer and diffuse alveolar hemorrhage/infection in vasculitis were also examined. As such, we retrospectively elaborated most likely CT features of each individual pathogen and briefly covered the differential diagnosis as well. Arguably, combination of pattern recognition with knowledge of the clinical setting could make a presumptive diagnosis and early treatment even more convenient. From the experience of first-line nephrologists, our work could make a substantial contribution to the expeditious and efficacious management of pulmonary infections in the pertinent patient population.

**Keywords:** kidney disease; hemodialysis; immunosuppression; pulmonary infections; computed tomography

## 1. Introduction

It is well known that patients on hemodialysis are more susceptible to infection than the general population since loss of renal function *per se* is an immunocompromised condition [1]. Both innate and adaptive immune systems are inevitably impaired by uremia in these patients [2]. Moreover, this uremia-associated immune impairment cannot be reversed by renal replacement therapy, including hemodialysis and kidney transplantation. Not surprising then, annual mortality rate secondary to sepsis was 100-300 folds higher in patients on dialysis than in the general population [3]. In fact, infections are an important cause of morbidity and mortality among patients at all stages of chronic kidney diseases and constitute the second most common cause of death in hemodialysis patients [4]. Furthermore, prolonged dialysis vintage markedly increased the risk of infection-related mortality than that of cardiovascular diseases-related one in long-term hemodialysis patients [5].

From a real-world practice perspective, respiratory tract infections are one of the most common types of infection in hemodialysis patients [6]. In this regard, incidence of



pneumonia among American patients on hemodialysis was 21.4 episodes per 100 patient-years, whereas 90.1% of the affected ones required hospital admission and 30-day mortality was 10.7% [7]. By comparison, access-related bloodstream infections are also common in hemodialysis patients, manifesting 7.7 episodes per 100 patient-years and respectively rendering hospitalizations and mortality rate of 48.0% and 1.6% [8]. At the same time, numerous novel immunosuppressive agents have been introduced in the treatment of immune-mediated kidney disease, which in turn have caused more opportunistic infections in the treated [9].

In an effort to secure our patients from these threats, we have previously reported opportunistic and severe infections caused by a full range of pathogens, zoonotic virus, nocardia and *Klebsiella pneumoniae* genus in immunocompromised patients with normal [10], impaired [11], loss of [12] renal function, and patients on maintenance hemodialysis [13], respectively. Of importance, our work clearly demonstrated that combination of CT image pattern recognition with knowledge of the clinical presentations was critical in initiating an expeditious treatment, a lesson that we have learnt in the hard way [11].

## 2. Materials and Methods

Following common practice [14], informed consent was not required as information was gathered by chart-image review, which is approved by our institutional review board.

### 2.1. Patients

The study was conducted as a multidisciplinary collaboration at the First Hospital of HeBei Medical University in northern China. We performed a retrospective study by reviewing the medical charts of the patients on maintenance hemodialysis (MHD) or under immunosuppressive therapy for primary membranous nephropathy (pMN) who were admitted for infection between February 2018 and August 2022. The descriptions for the MHD and pMN patients were elaborated previously in details [10, 13].

### 2.2. Definition of infection and identification of pathogens

Specifically, the infection was either airway invasive, when the causal organisms are identified deep into the airway basement membrane, or hematogenous spread, when there is invasion and occlusion of small arteries. Specific infections were diagnosed by evaluations of the clinical features, laboratory results, chest CT findings and, microbiological study including culture of sputum/blood/urine/catheter tip, serologic tests for likely pathogens, bronchoalveolar lavage (BAL) and metagenomics next generation sequencing when deemed appropriate [13].

### 2.3. Interpretation of CT imaging

CT imaging was interpreted by standard reporting procedure and cross-validated by senior clinicians of thoracic surgery and radiology. Accordingly, anomalous CT findings were defined as airspace consolidation; ground glass attenuation (GGA); tree-in-bud pattern; bronchial wall thickening; interlobular septal (ILS) thickening; crazy-paving pattern; mosaic pattern; nodules; halo sign; hilar or mediastinal lymph node (LN) enlargement and pleural effusion.

## 3. Results

Pictorially, the most common patterns seen at CT in acute pulmonary infections [15] are GGA, nodules, tree-in-bud appearance, consolidation or a combination of these findings (Figure 1). Clinically, major pathogens of pneumonia in MHD patients were *Klebsiella* (K.) *pneumoniae* and *Staphylococcus* (S.) *aureus* [6]. In case of *K. pneumoniae* pneumonia, CT findings consisted mainly of bilateral GGA, consolidation and intralobular reticular opacity (Figure 2A). In diabetic patients on hemodialysis [13], however, we found that BSI

caused by the hypervirulent *K. pneumoniae* may elicit pulmonary manifestations (Figure 2B) mimicking those of gram-positive cocci, as depicted hereafter.

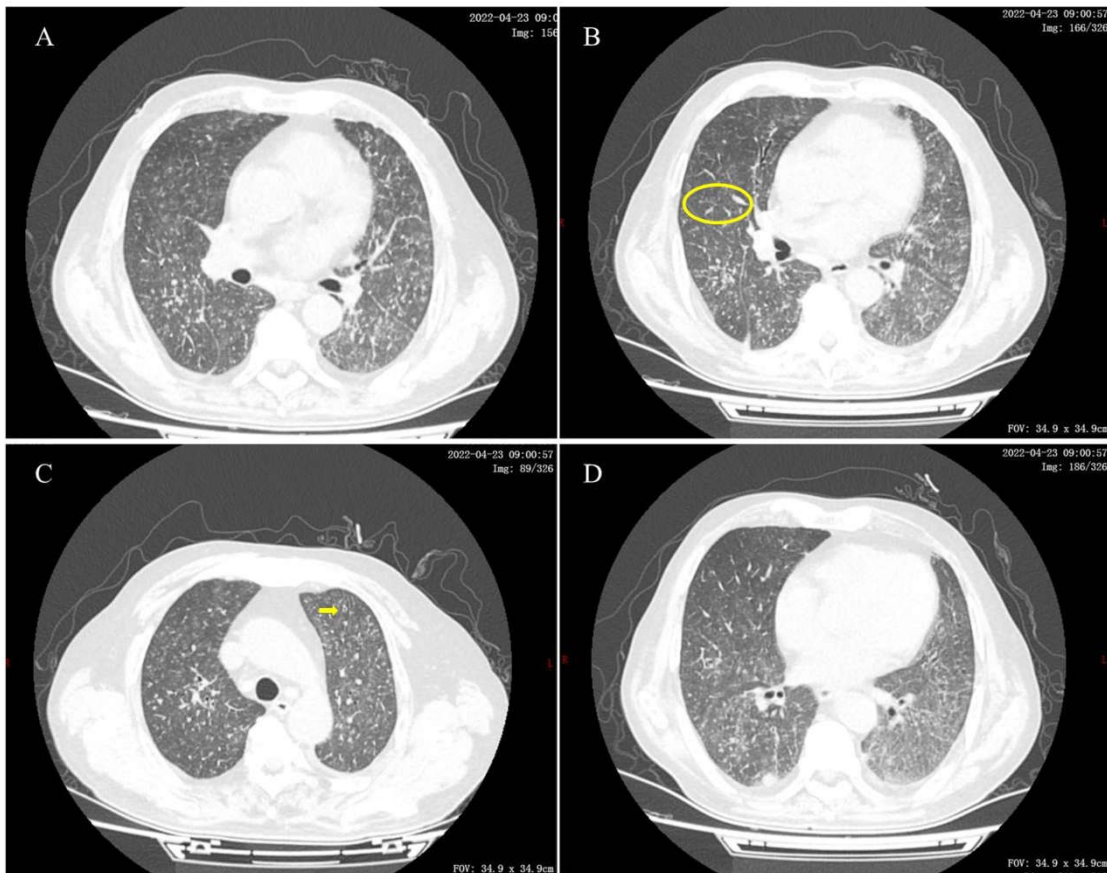


**Figure 1.** High-resolution CT showed diffuse bilateral pulmonary lesions in a 67-year-old febrile male with hypoxemia who had taken 3-month of cyclophosphamide and prednisone for primary membranous nephropathy, and developed steroid diabetes *ad interim*. The lesions included miliary centrilobular nodules indicative of bronchiolar infection (A), “tree-in-bud” appearance (circle, B) and thickening of bronchiolar walls (arrow, C). Ground-glass attenuation and consolidation were also visible (D).

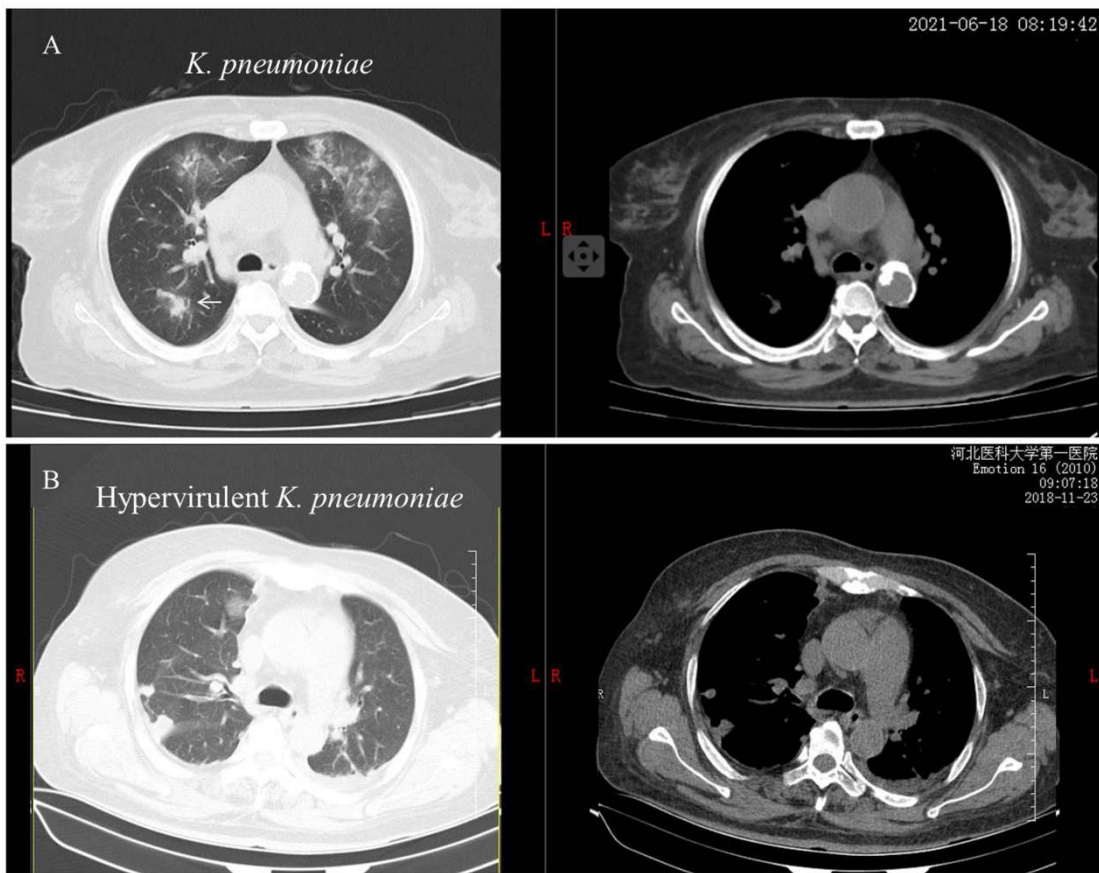


**Figure 2.** A 72-year-old female with fever and currant-jelly sputum had *Klebsiella pneumoniae* isolated from her blood. Chest CT scan found ground-glass attenuation, reticular opacity and bronchial wall thickening (arrow, A); A 55-year-old diabetic female on maintenance hemodialysis for 4.5 years admitted with an infected arteriovenous fistular. Numerous metastatic abscesses were found in which there were centrilobular nodules located peripherally on CT and hypervirulent *Klebsiella pneumoniae* was identified from her fingertip lesions by the mNGS (B).

Bloodstream infection in MHD patients was highlighted by the vascular access-related one, in which aerobic gram-positive cocci, *S. aureus* and methicillin-resistant *S. aureus* (MRSA) accounted for 85.3%, 36.8% and 10.0% of the causative pathogens, respectively (16). The most frequent CT findings in *S. aureus* pneumonia were GGA and bronchial wall thickening, followed by consolidation, centrilobular nodules and reticular opacity. In patients with MRSA infection, particularly, there were multiple parenchymal abnormalities mainly distributed peripherally (Figure 3A) with a higher propensity of pleural effusion, cavitation and empyema [17]. By comparison, centrilobular nodules, centrilobular nodules with a tree-in-bud pattern, and bronchial wall thickening were significantly more frequent in those with methicillin-susceptible *S. aureus* pneumonia (Figure 3B). With regard to the distinct bronchial wall thickening and centrilobular nodules on CT images, it is essentially important to know that bronchopneumonia with *S. aureus* infection differed pathogenetically from airspace pneumonia such as the one caused by *K. pneumoniae* in the production of a relatively small amount of fluid and by the rapid inflammatory exudation of numerous polymorphonuclear leukocytes.



**Figure 3.** A 33-year-old female admitted for infection of the central venous catheter that was used for hemodialysis. Peripheral nodular opacities with cavitation were visible (A) and blood culture identified methicillin-resistant *Staphylococcus aureus*; A 31-year-old female with skin puncture site infection near her arteriovenous fistula. Numerous centrilobular nodules and bronchial wall thickening (arrows) were demonstrated on CT (B). Blood culture isolated methicillin-susceptible *Staphylococcus aureus*.

Invasive fungal infections, most of which are due to *Aspergillus* and *Candida* species, are also a major cause of morbidity and mortality in our patients of interest. On chest CT, airway invasive aspergillosis typically manifests with multiple centrilobular nodules, tree-in-bud opacities, and peribronchovascular consolidation, which reflect the presence of bronchiolitis and bronchopneumonia. Alternatively, angioinvasive aspergillosis is characterized by the presence of single or multiple nodules, typically surrounded by a halo of GGA [18]. On the other hand, *candida* species are more prone to hematogenous spread which may manifest with miliary nodules or multiple larger nodules in a random distribution, whereas aspiration of contaminated oropharyngeal secretions may result in bronchopneumonia [19]. In addition, halo sign, cavitation, and ground-glass opacities may be present in both groups. Apparently, CT findings of pulmonary aspergillosis and candidiasis in the affected patients are similar. Histologically, however, pulmonary candidiasis tends to involve small blood vessels and have a random distribution and seldom leads to invasion and occlusion of large vessels, as commonly seen in invasive aspergillosis (Figure 4).

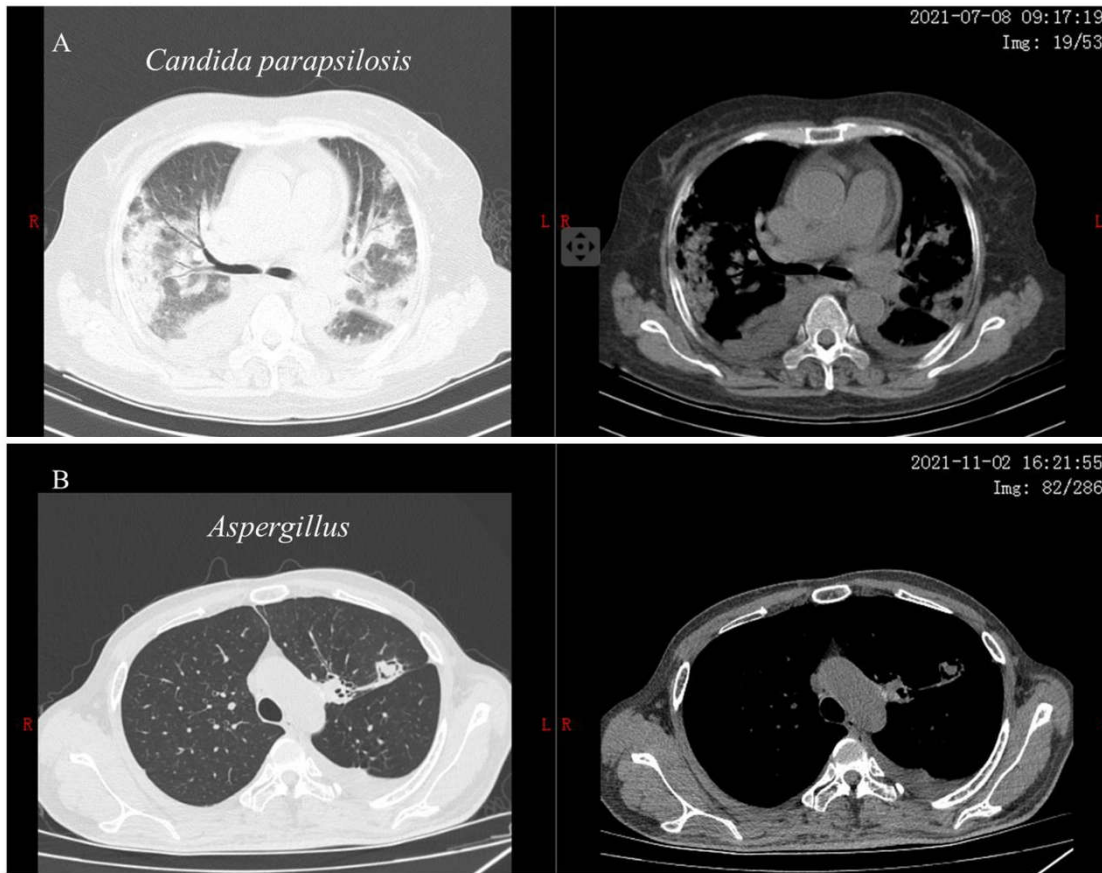


**Figure 4.** A 67-year-old female admitted for fever and infected artificial vascular graft. CT scan on arrival demonstrated bilateral multiple ill-defined nodules with cavitation and non-segmental consolidations (A). The diagnosis of *candida parapsilosis* infection was confirmed by culture of BAL; A 36-year-old diabetic male with nephrotic syndrome manifesting marked hypoalbuminemia. CT scan showed a 2.3cm mass within the left upper lobe with the air-crescent sign (B). The diagnosis of *Aspergillus* infection was confirmed by thoracoscopic biopsy.

Less encountered but with no less fatality, pulmonary infections caused by *Cryptococcus* and *Mucormycosis* deserve equal attention in our studied patients. In case of the pulmonary cryptococcosis, the most common CT findings are solitary or multiple nodules with or without cavitation in the subpleural areas of the lung (Figure 5A). Cavitation may be present in 30% of the patients who had nodules [20]. In term of morphology [21], pulmonary mucormycosis usually manifests as a mass or masses with a halo or reversed-halo sign on the initial CT scan followed by a decreased extent of surrounding ground-glass opacities with the development of internal necrosis during follow-up (Figure 5B). As imaging analogues, there were *pneumocystis jirovecii pneumonia* (PCP) and the one caused by *cytomegalovirus* (CMV) (Figure 6). For PCP, GGA was the predominant CT finding in 95.5-99.0% of the cases [22, 23], with the presence of a mosaic pattern and the absence of nodules as potential indicators [22], and subpleural sparing the unique feature [23]. With respect to the CMV pneumonia, CT manifestations usually consisted of a mixture of patterns, most commonly GGA with ill-defined demarcation, areas of consolidation, and small nodules [24]. Of note, CT findings of this viral pneumonia may be quite variable among different patient populations according to their disparate underlying diseases [25]. Purportedly, PCP and CMV pneumonia are often difficult to distinguish because of their clinical and radiological similarities [22]. Definite diagnosis, therefore, depends on the confluence of various clinical, etiological and radiographic patterns.

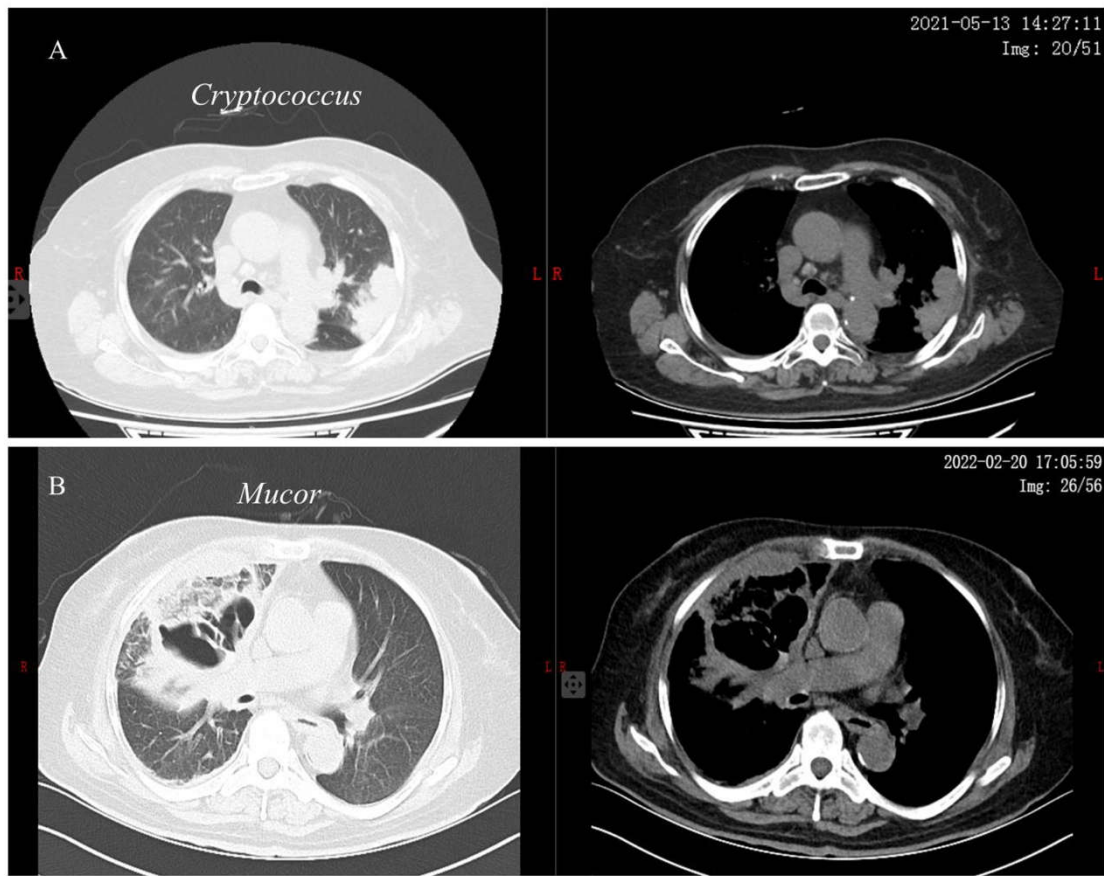


**Figure 5.** A 80-year old female was admitted for one week history of headache and fever, topping at 38.9 °C. Prior to this event, she had taken tacrolimus and prednisone for 7 months, treating primary membranous nephropathy. Chest CT scan found patchy areas of consolidation with adjacent ground-glass opacities in the subpleural region of the left upper lobe (A). *Cryptococcus* was subsequently identified from her sputum and cerebrospinal fluid; A 71-year-old female with stage V diabetic nephropathy was referred to us for one month history of cough, dyspnea and pleural chest pain. Chest CT scan showed masses with thick walled cavitation and the “reversed-halo” sign surrounded by ground-glass opacities (B). mNGS detected *mucorales* from the affected lung tissue obtained through bronchoscope.

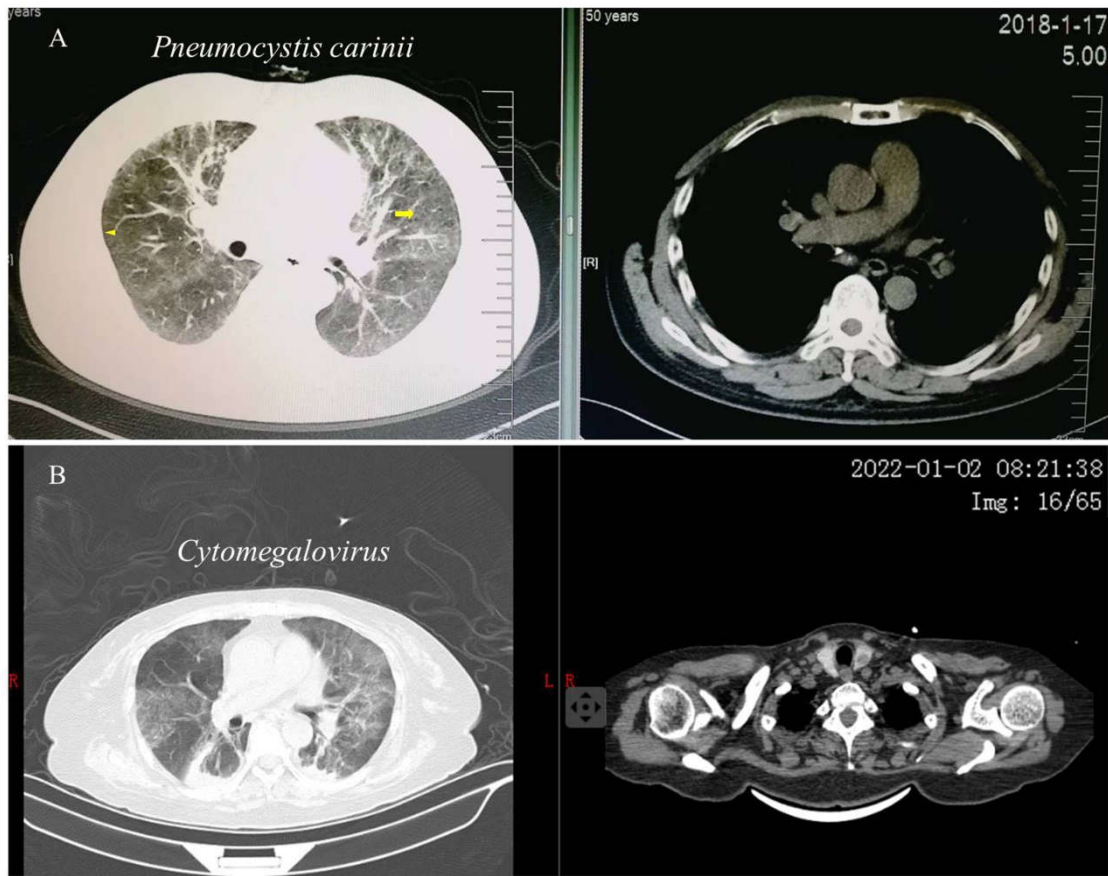


**Figure 6.** A 50-year old male was admitted for 2 day's fever of 39.2 °C, with dyspnea and non-productive cough. He had been taking cyclosporine and methylprednisolone for two month because of primary membranous nephropathy. Chest CT scan after admission showed bilateral ground-glass attenuation with a mosaic pattern (arrow, A), subpleural sparing was also visible but less discernible (arrowhead). The diagnosis of PCP was made by mNGS of his BAL; A 32-year-old male was feverish for one day, who had received kidney transplantation thirteen years ago and took mycophenolate mofetil, tacrolimus and prednisone thereafter. CT scan showed patchy areas of ground-glass attenuation (B). The diagnosis of MCV infection was confirmed by blood mNGS.

As uncommon as it is, pulmonary nocardiosis is an important cause of opportunistic infection in immunosuppressed patients and may develop fulminant trajectory resembling acute bacterial pneumonia. Under this circumstance, it is crucial to know that nocardia may likely produce metastatic spread, most commonly to the brain, because of its propensity for hematogenous dissemination as we have previously encountered [12]. Generally, this organism causes an acute, often necrotizing pneumonia, commonly associated with cavitation (Figure 7A). Other radiologic manifestations include nodules, reticulonodular or diffuse pneumonic infiltrates, single or multiple abscesses, that frequently abut on the pleural space [26]. However, these findings are non-specific and may often bear close resemblance to tuberculosis (Figure 7B), granulomatous diseases, or lung cancer. As for the pulmonary tuberculosis, major CT findings included segmental distribution (97%), satellite lesions (93%), single cavity within any given lesion (95%), and tendency toward architectural distortion and loss of volume [27]. Empirically, post-primary tuberculosis initially presents as an acute necrotizing pneumonia in the anterior segment of the upper lobes.

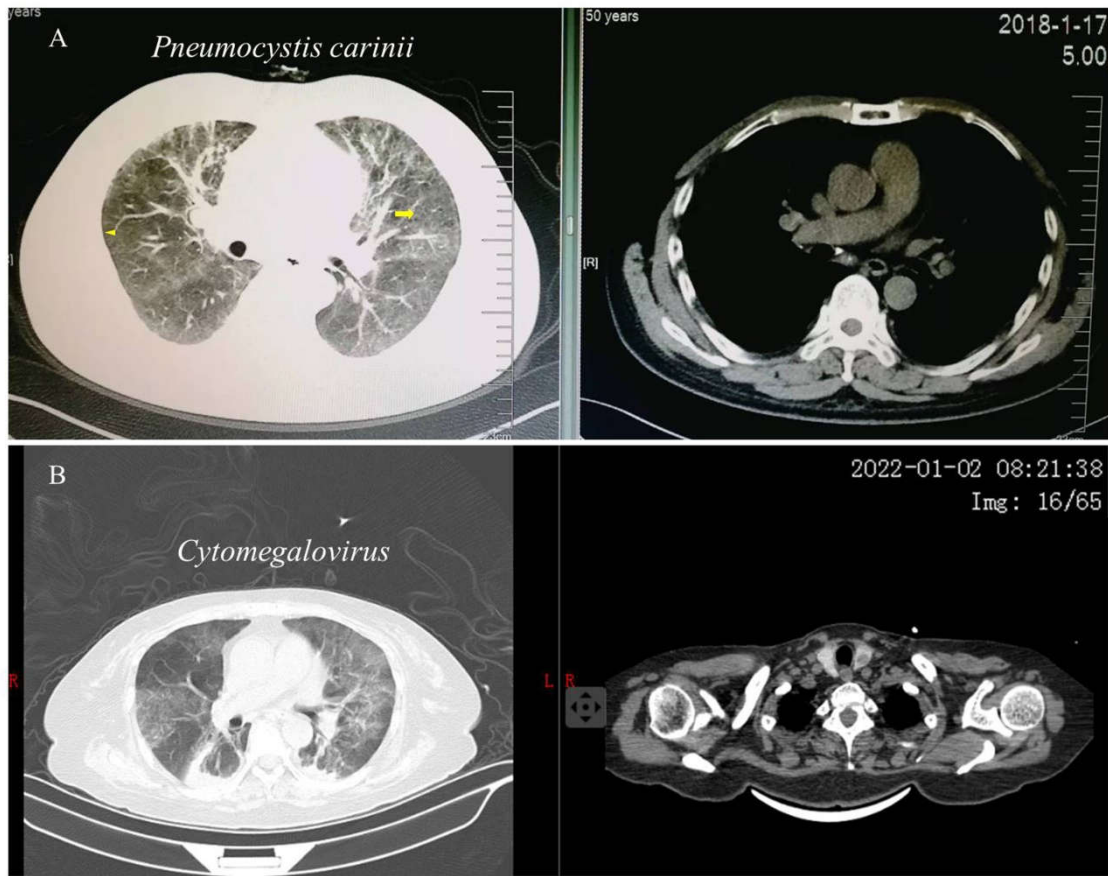


**Figure 7.** A 53-year-old female presented with fever of 38.6°C and hemoptysis for one day. She had previously received myethylprednisolone pulse therapy of 320mg for three consecutive days followed by routine daily dose of 40mg one month ago due to biopsy confirmed type III crescentic glomerulonephritis. CT scan found multiple polysized pulmonary nodules with cavitation (A) and growth of *Nocardia* asteroid from the sputum was found on the Loewenstein-Jensen media and subsequently confirmed by the 16S rDNA sequence analysis; A 52-year-old diabetic male with chronic kidney disease stage V claimed chest distress but was afebrile. CT scan showed multiple nodular lesions of various sizes with cavitations in the superior segment of right upper lobe (B). The diagnosis was a clinical one with positive acid-fast stain test of sputum smear.

Despite imaging similarities, pulmonary nodules in Wegener's granulomatosis were usually well demarcated and distributed mainly in the peripheral zone on CT scan (Figure 8A) [28]. In clinical setting, increased disease activity is almost inevitably accompanied by elevated anti-neutrophil cytoplasmic antibody (ANCA) titer (predominantly anti-proteinase 3) and aggravated target organ damage. Likewise, malignancy should be considered in nodules with irregular, lobulated, or spiculated borders (Figure 8B) as discussed most recently [29]. Arguably, diffuse alveolar hemorrhage (DAH) cannot be left out when sorting out pulmonary infection in immunocompromised patients. Currently, we only covered DAH in autoimmune kidney diseases exemplified by ANCA-associated vasculitis and those secondary to diverse etiologies including infection could be found elsewhere [30]. CT findings in early DAH are characterized by pulmonary opacities with varying degrees of ground-glass opacity and consolidation (Figure 9A). These abnormalities may progress to thickening of bronchovascular bundles, honey-combing and, in the worst scenario, crazy-paving pattern [31]. The differential diagnosis of CT imaging findings in DAH most broadly overlaps with pulmonary edema and infections (Figure 9B). When suspecting infectious etiologies, clinical presentation and laboratory data such as fever, cough, and specific infectious markers may provide supportive clues [32]. However, there are considerable perplexing cases of DAH indistinguishable from infections and *vice versa*. In these cases, BAL may be the proper option.

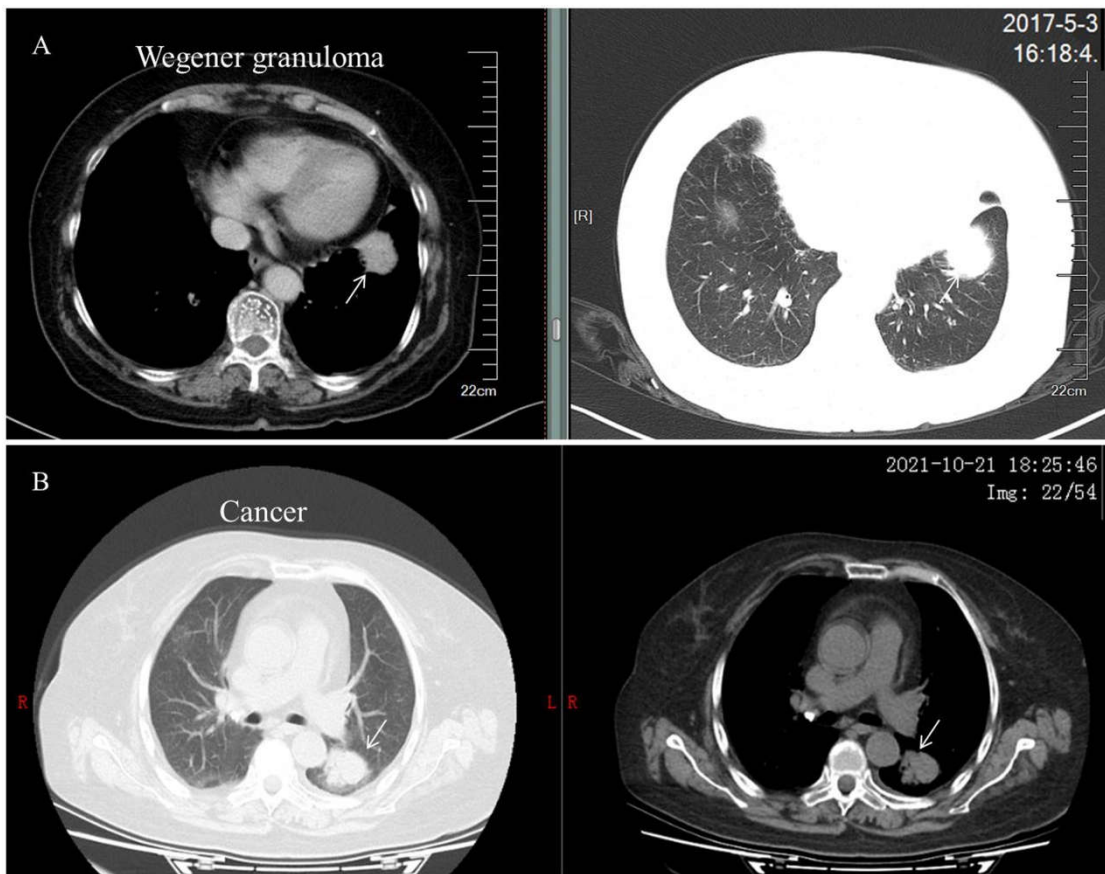


**Figure 8.** A 72-year-old female with a biopsy-proven renal crescent glomerulonephritis. Her anti-proteinase 3 ANCA was strongly positive and medium-enhanced CT scan found a lobulated and spiculated soft tissue nodule with irregular border in the posterior basal segment of the right lower lobe (arrow, A), which was eventually identified as Wegener's granulomatosis by bronchoscope; A 66-year-old female presented with acute kidney injury of two days. CT scan showed narrowed bronchial space of the dorsal segment in the left lower lobe surrounded by an irregular mass (arrow, B), which was confirmed as malignant by CT-guided percutaneous needle aspiration.

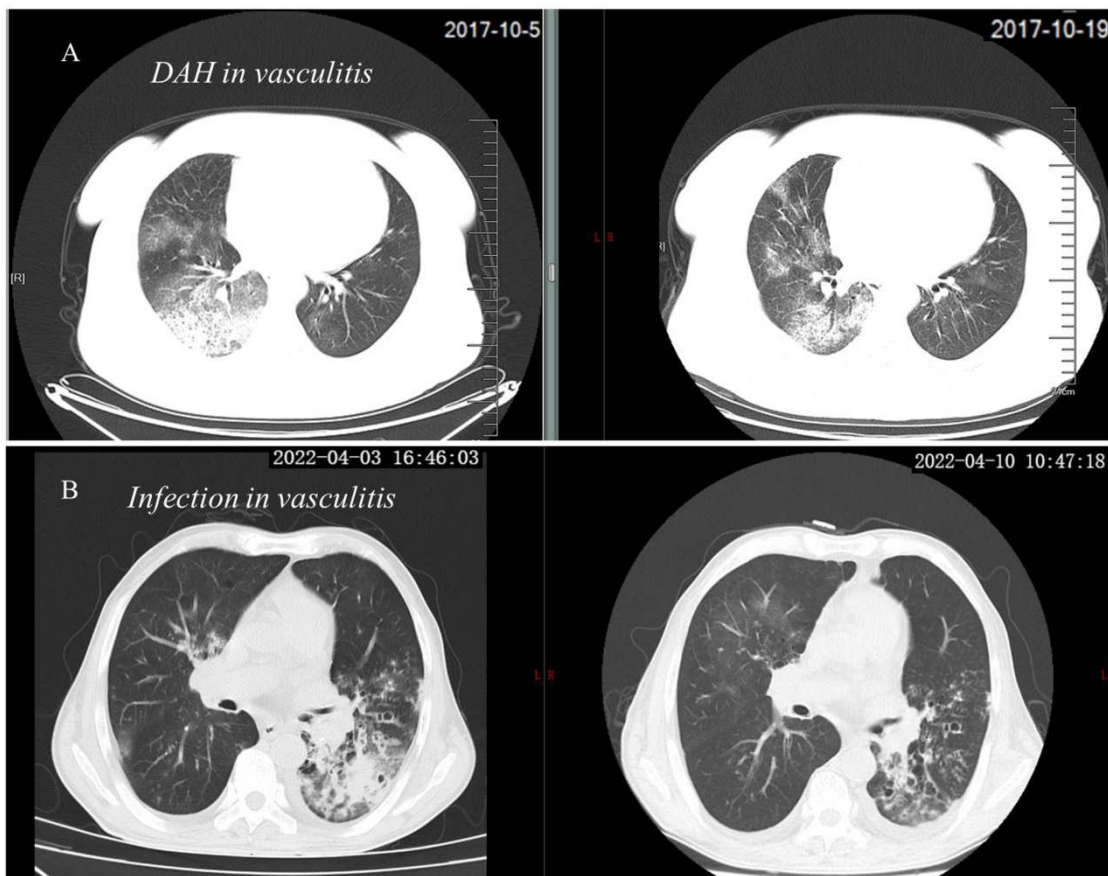


**Figure 9.** A 72-year-old afebrile female was admitted for anuria acute renal failure accompanied by hemoptysis. Her renal biopsy-assisted clinical diagnosis was ANCA (myeloperoxidase)-associated microscopic polyangiitis and diffuse alveolar hemorrhage. CT scan showed unilateral pulmonary ground-glass and honey-combing opacities (A), which was greatly mitigated after a therapeutic regime of plasmapheresis and myethylprednisolone pulse therapy 14-days later; A 67-year-old male claimed fever, productive cough and general malaise for one week. His renal lesion was the same with above-mentioned female patient and his chest CT imaging was consistent with bronchiectasis with infection (B), which was remarkably alleviated after the use of antibiotics for one week.

With respect to the predominant CT pattern in each infection, segmental GGA/Consolidation in bacterial pneumonia (61.0%), nodules of small size (22.5%) and large size (31.3%) in fungal infections, diffuse GGA in PCP (81.0%) and CMV pneumonia (63.6%), and nodules of small size (53.3%) in TB were significantly more prevalent as summarized by Kunihiro *et al* [22]. Nevertheless, these observations should be interpreted with great caution as there is no unique pattern for one specific pathogen and the infection is usually sprouted as mixed in the susceptible patients. Furthermore, infection inherently depends on the patient's immune status and the risk of opportunistic infections may also change over time.

#### 4. Conclusion

Identification of the causative pathogen(s) relies on the clinician's recognition combined with clinical, laboratory, immunological and radiologic features. Early recognition is crucial as prompt diagnosis and treatment are required for patients' survival and our work may cogently contribute to this demanding requirement.

**Author Contributions:** Conceptualization and methodology, T.W.; investigation, S.Z., X.M.L.; data curation, X.M.L.; CT image interpretation, H.N.L., Y. W.; original draft preparation, S.Z.; review and editing, T.W., L.H.Z.; coordination, P.H.H. All authors have read and agreed to the published version of the manuscript.

**Funding:** This research received no external funding.

**Institutional Review Board Statement:** The study was conducted in accordance with the Declaration of Helsinki and was approved by the First Hospital of HeBei Medical University Ethics Committee and date of approval: 03 March 2022.

**Informed Consent Statement:** Since this was a retrospective study, the Ethics Committee waived the need for an informed consent, and a policy of strict anonymity and confidentiality was assured.

**Data Availability Statement:** The data presented in this study are available on request from the corresponding author.

**Acknowledgments:** None

**Conflicts of Interest:** The authors declare no conflict of interest.

## References

1. Bello, A.K.; Okpechi, I.G.; Osman, M.A.; Cho, Y.; Htay, H.; Jha, V.; Wainstein, M.; Johnson, D.W. Epidemiology of Haemodialysis Outcomes. *Nat Rev Nephrol* **2022**, *18*, 378-395.
2. Syed-Ahmed, M.; Narayanan, M. Immune Dysfunction and Risk of Infection in Chronic Kidney Disease. *Adv Chronic Kidney Dis* **2019**, *26*, 8-15.
3. Sarnak, M.J.; Jaber, B.L. Mortality Caused by Sepsis in Patients with End-Stage Renal Disease Compared with the General Population. *Kidney Int* **2000**, *58*, 1758-1764.
4. Hiyamuta, H.; Yamada, S.; Taniguchi, M.; Nakano, T.; Tsuruya, K.; Kitazono, T. Causes of Death in Patients Undergoing Maintenance Hemodialysis in Japan: 10-Year Outcomes of the Q-Cohort Study. *Clin Exp Nephrol* **2021**, *25*, 1121-1130.
5. Sumida, K.; Yamagata, K.; Iseki, K.; Tsubakihara, Y. Different Impact of Hemodialysis Vintage on Cause-Specific Mortality in Long-Term Hemodialysis Patients. *Nephrol Dial Transplant* **2016**, *31*, 298-305.
6. Berman, S.J.; Johnson, E.W.; Nakatsu, C.; Alkan, M.; Chen, R.; LeDuc, J. Burden of Infection in Patients with End-Stage Renal Disease Requiring Long-Term Dialysis. *Clin Infect Dis* **2004**, *39*, 1747-1753.
7. Sibbel, S.; Sato, R.; Hunt, A.; Turenne, W.; Brunelli, S.M.; The Clinical and Economic Burden of Pneumonia in Patients Enrolled in Medicare Receiving Dialysis: A Retrospective, Observational Cohort Study. *BMC Nephrol* **2016**, *17*, 199.
8. Nguyen, D.B.; Shugart, A.; Lines, C.; Shah, A.B.; Edwards, J.; Pollock, D.; Sievert, D.; Patel, P.R. National Healthcare Safety Network (NHSN) Dialysis Event Surveillance Report for 2014. *Clin J Am Soc Nephrol* **2017**, *12*, 1139-1146.
9. Kant, S.; Kronbichler, A.; Sharma, P.; Geetha, D. Advances in Understanding of Pathogenesis and Treatment of Immune-Mediated Kidney Disease: A Review. *Am J Kidney Dis* **2022**, *79*, 582-600.
10. Wang, T.; Zhang, Y.; Ping, F.; Zhao, H.; Yan, L.; Lin, Q.; Zhang, H. Predicting Risk of Pulmonary Infection in Patients with Primary Membranous Nephropathy on Immunosuppressive Therapy: The AIM-7C Score. *Nephrology (Carlton)* **2019**, *24*, 1009-1016.
11. Zhang, Y.; Hu, M.; Wei, D.; Zhang, H.; Chu, B.; Xu, H.-M.; Wang, T. From Severe Herpes Zoster to Rare Suid Herpesvirus Encephalitis: A New Twist of the Varicellovirus Genus Infection in Patients with Kidney Diseases. *Int J Med Sci* **2020**, *17*, 745-750.
12. Wang, T.; Jia, Y.; Chu, B.; Liu, H.; Dong, X.; Zhang, Y. Nocardiosis in Kidney Disease Patients under Immunosuppressive Therapy: Case Report and Literature Review. *Int J Med Sci* **2019**, *16*, 838-844.
13. Zhou, S.; Ren, G.; Liu, Y.; Liu, X.; Zhang, L.; Xu, S.; Wang, T. Challenge of Evolving Klebsiella Pneumoniae Infection in Patients on Hemodialysis: From the Classic Strain to the Carbapenem-Resistant Hypervirulent One. *Int J Med Sci* **2022**, *19*, 416-424.
14. Ahmad, S.B.; Santoriello, D.; Canetta, P.; Bomback, A.S.; D'Agati, V.D.; Markowitz, G.; Ahn, W.; Radhakrishnan, J.; Appel, G.B. Concurrent Anti-Glomerular Basement Membrane Antibody Disease and Membranous Nephropathy: A Case Series. *Am J Kidney Dis* **2021**, *78*, 219-225.e1.
15. Sharma, S. Computed Tomography for the Diagnosis of Infectious Diseases of the Chest. *Expert Opin Med Diagn* **2008**, *2*, 1247-1262.
16. Taylor, G.; Gravel, D.; Johnston, L.; Embil, J.; Holton, D.; Paton, S.; Canadian Hospital Epidemiology Committee. Canadian Nosocomial Infection Surveillance Program Prospective Surveillance for Primary Bloodstream Infections Occurring in Canadian Hemodialysis Units. *Infect Control Hosp Epidemiol* **2002**, *23*, 716-720.
17. Zhang, Y.; Wang, H.-B.; Chu, B.; Zhao, H.-Z.; Li, H.; Zhou, H.-M.; Wang, T. Disparate Effects of Methicillin-Resistant Staphylococcus Aureus Infection on Renal Function in IgA-Dominant Infection-Associated Glomerulonephritis and Menstrual Toxic Shock Syndrome: A Case Report and Literature Review. *J Int Med Res* **2020**, *48*, 300060520933810.
18. Althoff Souza, C.; Müller, N.L.; Marchiori, E.; Escuissato, D.L.; Franquet, T. Pulmonary Invasive Aspergillosis and Candidiasis in Immunocompromised Patients: A Comparative Study of the High-Resolution CT Findings. *J Thorac Imaging* **2006**, *21*, 184-189.

19. Franquet, T.; Müller, N.L.; Lee, K.S.; Oikonomou, A.; Flint, J.D. Pulmonary Candidiasis after Hematopoietic Stem Cell Transplantation: Thin-Section CT Findings. *Radiology* **2005**, *236*, 332-337.

20. Kishi, K.; Homma, S.; Kurosaki, A.; Kohno, T.; Motoi, N.; Yoshimura, K. Clinical Features and High-Resolution CT Findings of Pulmonary Cryptococcosis in Non-AIDS Patients. *Respir Med* **2006**, *100*, 807-812.

21. Choo, J.Y.; Park, C.M.; Lee, H.-J.; Lee, C.H.; Goo, J.M.; Im, J.-G. Sequential Morphological Changes in Follow-up CT of Pulmonary Mucormycosis. *Diagn Interv Radiol* **2014**, *20*, 42-46.

22. Kunihiro, Y.; Tanaka, N.; Kawano, R.; Yujiri, T.; Kubo, M.; Ueda, K.; Gondo, T.; Kobayashi, T.; Matsumoto, T.; Differential diagnosis of pulmonary infections in immunocompromised patients using high-resolution computed tomography. *Eur Radiol* **2019**, *29*, 6089-6099.

23. Obmann, V.C.; Bickel, F.; Hosek, N.; Ebner, L.; Huber, A.T.; Damonti, L.; Zimmerli, S.; Christe, A. Radiological CT Patterns and Distribution of Invasive Pulmonary Aspergillus, Non-Aspergillus, Cryptococcus and Pneumocystis Jirovecii Mold Infections - A Multicenter Study. *Rofo* **2021**, *193*, 1304-1314.

24. Franquet, T.; Lee, K.S.; Müller, N.L. Thin-Section CT Findings in 32 Immunocompromised Patients with Cytomegalovirus Pneumonia Who Do Not Have AIDS. *AJR Am J Roentgenol* **2003**, *181*, 1059-1063.

25. Omeri, A.K.; Okada, F.; Takata, S.; Ono, A.; Nakayama, T.; Ando, Y.; Sato, H.; Hiramatsu, K.; Mori, H. Comparison of High-Resolution Computed Tomography Findings between *Pseudomonas Aeruginosa* Pneumonia and Cytomegalovirus Pneumonia. *Eur Radiol* **2014**, *24*, 3251-3259.

26. Yildiz, O.; Doganay, M. Actinomycoses and Nocardia Pulmonary Infections. *Curr Opin Pulm Med* **2006**, *12*, 228-234.

27. Ikezoe, J.; Takeuchi, N.; Johkoh, T.; Kohno, N.; Tomiyama, N.; Kozuka, T.; Noma, K.; Ueda, E. CT Appearance of Pulmonary Tuberculosis in Diabetic and Immunocompromised Patients: Comparison with Patients Who Had No Underlying Disease. *AJR Am J Roentgenol* **1992**, *159*, 1175-1179.

28. Blum, U.; Windfuhr, M.; Buitrago-Tellez, C.; Sigmund, G.; Herbst, E.W.; Langer, M. Invasive Pulmonary Aspergillosis. MRI, CT, and Plain Radiographic Findings and Their Contribution for Early Diagnosis. *Chest* **1994**, *106*, 1156-1161.

29. Mazzone, P.J.; Lam, L. Evaluating the Patient With a Pulmonary Nodule: A Review. *JAMA* **2022**, *327*, 264-273.

30. Escuissato, D.L.; Warszawiak, D.; Marchiori, E. Differential Diagnosis of Diffuse Alveolar Haemorrhage in Immunocompromised Patients. *Curr Opin Infect Dis* **2015**, *28*, 337-342.

31. Collins, C.E.; Quismorio, F.P. Pulmonary Involvement in Microscopic Polyangiitis. *Curr Opin Pulm Med* **2005**, *11*, 447-451.

32. Lichtenberger, J.P.; Digumarthy, S.R.; Abbott, G.F.; Shepard, J.-A.O.; Sharma, A. Diffuse Pulmonary Hemorrhage: Clues to the Diagnosis. *Curr Probl Diagn Radiol* **2014**, *43*, 128-139.